# Microscopic analysis of the $^6$Li($^6$Li, $^6$Li*(3.56))$^6$Li*(3.56) and the $^6$Li($^6$Li, $^6$He)$^6$Be reactions*

W. R. Wharton
*Department of Physics, University of Washington, Seattle, Washington 98195*
(Received 13 July 1973)

A microscopic distorted-wave Born-approximation (DWBA) analysis of the $^6$Li-($^6$Li, $^6$Li*(3.56))$^6$Li*(3.56) and the $^6$Li($^6$Li, $^6$He)$^6$Be reactions has been made and compared to microscopic studies of the $(p,p')$ and $(^3\mathrm{He},t)$ reactions. The tensor interaction and full exchange of the $1p$ shell nucleons has been included. Agreement between the calculation and the data is generally good with two exceptions, and this agreement suggests that the reactions are indeed quasielastic. Special emphasis is given toward explaining the differences between the measured $^6$Li($^6$Li, $^6$Li*(3.56))$^6$Li*(3.56) and $^6$Li($^6$Li, $^6$He)$^6$Be cross sections. The cross sections should be equal according to charge independence because all final states are members of the same $T=1$ isomultiplet. The theory correctly predicts the angular dependence of the difference in the two cross sections, but it does not predict the magnitude of the difference. The source of this disagreement may be attributed to differences in the wave functions of the final nuclei which are difficult to calculate.

[ NUCLEAR REACTIONS $^6$Li($^6$Li, $^6$Li), ($^6$Li, $^6$Li*(3.56)), ($^6$Li, $^6$He), $E=28$–$36$ MeV; calculated $\sigma(E,\theta)$; deduced optical-model parameters. Microscopic DWBA analysis, deduced charge dependence. ]

During the last several years there has been considerable effort[1] to describe inelastic and charge-exchange reactions such as $(p,p')$ and $(^3\mathrm{He},t)$ with part or all of the interaction treated microscopically using a realistic effective nucleon-nucleon interaction, $V_{\mathrm{eff}}$. A microscopic analysis requires an accurate description of $V_{\mathrm{eff}}$, the reaction mechanism, and the initial and final nuclear states. It is not always clear, such as in the $(^3\mathrm{He},t)$ reaction,[2] which of these are at fault for causing some disagreement between the theory and the experiment. There are also approximations within the distorted-wave Born-approximation (DWBA) theory which may be more serious for certain types of reactions. It is therefore interesting to apply the microscopic theory to other reactions and try to obtain a consistent decription using the same $V_{\mathrm{eff}}$. In this report the $^6$Li($^6$Li, $^6$He)$^6$Be and the $^6$Li($^6$Li, $^6$Li*)$^6$Li* reactions (where $^6$Li* designates the state at 3.56 MeV excitation in $^6$Li) have been subjected to a partial microscopic analysis. These reactions have been tentatively characterized as "quasielastic," double-spin–isospin-flip, zero orbital angular momentum transfer reactions[3–5] involving only the direct interaction of a $p$-shell valence nucleon in each nucleus. This description has already been used[5] with some success in a microscopic analysis of the $^6$Li($^6$Li, $^6$Li*)$^6$Li* reaction. All states involved in these reactions are well described by $l$-$s$ coupling where there are 4 nucleons filling the $1s$ shell and 2 $1p$ nucleons coupled to $l=0$, $s=1$, $T=0$ in the $^6$Li ground state and $l=0$, $s=0$, $T=1$ in the final states.[6] Because the initial and final states have identical configurations except for the spin and isospin coupling of the $1p$ shell nucleons, a quasielastic process appears most likely.

There are several problems which make the study of the $^6$Li($^6$Li, $^6$Li*)$^6$Li* and the $^6$Li($^6$Li, $^6$He)-$^6$Be reactions difficult. A major problem with any reaction is that it is necessary to antisymmetrize the nucleons in the projectile with the nucleons in the target and this means the inclusion of exchange terms. To date most microscopic calculations have included only the exchange of the two interacting nucleons, commonly referred to as the "knock-on" exchange terms. For $(p,p')$ it can be argued that this so-called knock-on exchange term is the only important exchange term since exchange terms involving the exchange of noninteracting nucleons require the overlap of a bound-state wave function with an unbound wave function. If the distorting potential is chosen to be energy-independent and real the overlap is zero resulting in no contribution from these other exchange terms. For complex projectiles this is no longer true. Exchange terms involving a non-interacting nucleon result in the noninteracting nucleon originating in the target and ending up in the projectile, or vice versa. The wave functions describing the nucleon in the target and projectile are generally not orthogonal and the contributions from such exchange terms may be significant. Clearly the problem is amplified the heavier the

projectile is, since there will be more nucleons to exchange. In this report all exchange terms between the $p$-shell nucleons have been included in the microscopic calculation. Unfortunately the inclusion of such exchange terms results in complicated calculations and some approximations must be made. Furthermore, the DWBA description of the scattering does not treat exchange terms correctly[7] and as such terms become more important the DWBA theory may be unsatisfactory. There is another problem with exchange terms. One would ideally like to isolate various terms of $V_{\text{eff}}$ and study them separately. This could be done by choosing reactions with certain selection rules which limit the pertinent interaction to a few terms of $V_{\text{eff}}$. For example, if the $^6$Li($^6$Li, $^6$Li*)$^6$Li* reaction is a one-step process then the Majorana term is the only part of the central potential that contributes to the reaction. In reality if exchange terms are included such a procedure is impossible because all terms of $V_{\text{eff}}$ will always contribute through the exchange terms. To calculate the exchange terms one commonly assumes certain relationships between the various parts of $V_{\text{eff}}$. For example, in this work a Serber potential will be assumed. The Serber potential is a fair approximation of the $N$-$N$ interaction and it assumes there is no interaction in the odd momentum states which is approximately true at low energies.[8]

There are other major problems with the analysis of the $^6$Li($^6$Li, $^6$Li*)$^6$Li* and the $^6$Li($^6$Li, $^6$He)$^6$Be reaction. For example, an optical potential is used to obtain the distorted-wave functions, but unfortunately the $^6$Li + $^6$Li elastic scattering has not been adequately analyzed to obtain a good optical potential. The basic question of how well the optical potential is capable of describing the $^6$Li + $^6$Li elastic scattering has not been properly answered.

Fortunately there are symmetry properties which make the analysis easier. The $^6$Li($^6$Li, $^6$Li*)-$^6$Li* reaction is unusual in that there are identical particles in the incoming channel and the outgoing channel. This means that both the incoming and outgoing channels obey Bose-Einstein statistics requiring the total wave functions to be symmetric in the exchange of the two nuclei. If the channel spin, $\vec{S}$, is defined as the vector sum of the intrinsic spins of the two nuclei, $\vec{S} = \vec{I} + \vec{I}'$, and $L$ is defined as the angular momentum of the relative motion of the nuclei, and $T_c$ is defined as the total isospin, $\vec{T}_c = \vec{T} + \vec{T}'$, then Table I gives the possible combinations of $L$, $S$, and $T_c$ that are allowed for the incoming and outgoing channels.

According to parity conservation, the reaction can proceed only when the incoming channel has even angular momentum and this further restricts the incoming channel to $S = 0$ or 2. The channel spin is approximately a good quantum number. To mix states of different channel spin, it is necessary to have spin-dependent second-rank tensor potentials which will mix $S = 0$ and 2. Such terms have been studied in the optical potential for deuteron scattering and are found to be present but weak.[9] In this study, the tensor terms are not included in the optical potential. With this approximation channel spin is a good quantum number and the central and tensor parts of $V_{\text{eff}}$ contribute incoherently to the cross section. The contribution of the central part of $V_{\text{eff}}$ to the reaction can come only from the $S = 0$ initial state since these terms commute with $S$. The contribution of the tensor part of $V_{\text{eff}}$ can come only from the $S = 2$ initial state. This incoherence is an advantage in the attempt to study the various parts of $V_{\text{eff}}$. However because the tensor terms are not included in the optical potential, one can at most make qualitative statements about the tensor potential in $V_{\text{eff}}$.

All the above statements also apply to the $^6$Li-($^6$Li.$^6$He)$^6$Be reaction according to charge independence. In fact if charge independence is completely valid then the cross sections are equal regardless of the reaction mechanism

$$\frac{d\sigma(^6\text{Li}(^6\text{Li}, ^6\text{Li}^*)^6\text{Li}^*)}{d\sigma(^6\text{Li}(^6\text{Li}, ^6\text{He})^6\text{Be})} = \left| \frac{\langle 1100 | 00 \rangle}{\langle 111-1 | 00 \rangle} \right|^2 = 1 ,$$

where the Clebsch-Gordan coefficients couple the isospin states of the outgoing nuclei to total isospin $T_c = 0$.

In actuality the scattering amplitudes should be somewhat charge-dependent. The $Q$ values for the two reactions are different. The Coulomb interactions in the outgoing channels are different, and the spatial wave functions of the final nuclei are different. Both $^6$He and $^6$Li*(3.56) are particle stable and $^6$Be is unstable to $\alpha + 2p$ decay. With charge dependence present there are also some changes in the selection rules of the $^6$Li($^6$Li, $^6$He)-$^6$Be reaction. In particular, through some charge-

TABLE I. Allowed states for the $^6$Li($^6$Li, $^6$Li*)$^6$Li* reaction.

| Channel spin | Incoming channel $T_c = 0$ | Outgoing channel $T_c = 0$ or 2 [a] |
|---|---|---|
| $S = 0$ | even $L$ | even $L$ |
| $S = 1$ | odd $L$ (parity forbidden) | ... |
| $S = 2$ | even $L$ | ... |

[a] Two $^6$Li*(3.56) nuclei cannot couple to $T_c = 1$. $T_c = 2$ will not occur if charge independence is valid.

dependent mechanism it is possible for the final nuclei $^6$He and $^6$Be to couple to total isospin $T_c = 1$. In this situation they will be in an odd angular momentum state and the contribution to such a configuration must come from the $S = 1$ state in the initial channel. It would be very surprising, however, if such a contribution to the cross section were measurable because it must add incoherently with the much larger charge-independent cross section. (The incoherence results from the restriction that the cross section be symmetric about 90° c.m.)

Considerable emphasis will be placed upon the comparison of the $^6$Li($^6$Li, $^6$Li*)$^6$Li* and the $^6$Li-($^6$Li.$^6$He)$^6$Be reactions, because presumably the $Q$ value and Coulomb effects can be accurately calculated, and any other charge-dependent effects will be of great interest.

## I. MICROSCOPIC DWBA THEORY

The microscopic DWBA used in these calculations has been given in considerable detail elsewhere,[7] and the theory will be reviewed only briefly here. It is assumed that each nucleus in these reactions is composed of three distinct particles: an $\alpha$ particle with two $p$-shell nucleons bound to it. The four nucleons are properly antisymmetrized resulting in six DWBA amplitudes representing a direct contribution and five exchange contributions. Only one of the five exchange contributions is the so-called knock-on exchange term involving the exchange of interacting nucleons. The wave functions describing the relative motion of the $^6$Li nuclei are also properly symmetrized to give the restrictions listed in Table I.

The usual DWBA approximations are made. The distorted waves are chosen to be wave functions generated from an optical potential and adjusted to fit the elastic scattering data. These distorted waves are not properly antisymmetrized with respect to the exchange of nucleons between the two nuclei and this leads to a violation of time-reversal invariance for some of the exchange terms involving noninteracting nucleons. More specifically there is no longer post-prior equivalence. Fortunately, in this work, the violation of post-prior equivalence does not appear to be sufficiently severe to restrict any of the conclusions or to seriously affect the calculated cross sections.

In calculating the exchange contribution the no-recoil approximation is made. More specifically the distance, $R$, between the centers of mass of the two nuclei is made to be independent of the exchanged $p$-shell nucleons. This assumes that the $\alpha$ particle is much more massive than the $p$-shell nucleons and leads to an overestimation of the exchange terms of about 15–20% according to a crude calculation.[5] With these approximations the total amplitude for going to channel $s, t$ is:

$$G_{st}(\theta, \phi) = \frac{-M}{2\pi\hbar^2} \int \upsilon^{-}_{\text{opt}}(\vec{R}) F(\vec{R}) \upsilon^{+}_{\text{opt}}(\vec{R}) d\vec{R},$$

where $\upsilon_{\text{opt}}(\vec{R})$ is the distorted wave and the form factor $F(\vec{R})$ can be written in either the post or prior representation:

$$F_{\text{post}}(R) = \langle U_s(1,2) U'_t(3,4) | \upsilon | A U_0(1,2) U'_0(3,4) \rangle,$$

and

$$F_{\text{prior}}(R) = \langle A U_s(1,2) U'_t(3,4) | \upsilon | U_0(1,2) U'_0(3,4) \rangle,$$

where the internal wave functions of the two nuclei (primed and unprimed) are denoted by $U(i,j)$. The subscript 0 denotes the $^6$Li ground state and $s, t$ the two final states. The four nucleons are labeled (1, 2, 3, 4) and the antisymmetrizer is

$$A = 1 - P_{13} - P_{14} - P_{23} - P_{24} + P_{13}P_{24}.$$

The interaction potential is defined as

$$\upsilon = \sum_{i=1}^{2} \sum_{j=3}^{4} V_{\text{eff}}(i,j),$$

where

$$V_{\text{eff}}(i,j) = V_c(\vec{r}_i - \vec{r}_j)[-3 + \vec{\sigma}_i \cdot \vec{\sigma}_j + \vec{\tau}_i \cdot \vec{\tau}_j + (\vec{\sigma}_i \cdot \vec{\sigma}_j)(\vec{\tau}_i \cdot \vec{\tau}_j)] + V_T(\vec{r}_i - \vec{r}_j)[-1 + \vec{\tau}_i \cdot \vec{\tau}_j] S_{12}(i,j),$$

and

$$S_{12}(i,j) = 3(\vec{\sigma}_i \cdot \hat{r}_{ij})(\vec{\sigma}_j \cdot \hat{r}_{ij}) - \vec{\sigma}_i \cdot \vec{\sigma}_j.$$

The form factor is defined such that it is nearly the same for the $^6$Li($^6$Li, $^6$Li*)$^6$Li* and $^6$Li($^6$Li, $^6$He)-$^6$Be reactions. The cross section of each reaction is

$$\left[\frac{d\sigma}{d\Omega}(\theta) + \frac{d\sigma}{d\Omega}(\pi - \theta)\right] = \frac{k_f}{k_i} \frac{1}{9} \sum_{I} \sum_{I'} [G(\theta, \phi) + G(\pi - \theta, \phi)]^2,$$

where we have averaged over the initial spins $I, I'$.

During the actual measurement $^6$He and $^6$Be are distinguishable and the $^6$Li($^6$Li, $^6$Li*)$^6$Li* measured cross section is approximately a factor 2 larger than the $^6$Li($^6$Li, $^6$He)$^6$Be cross section

$$\frac{d\sigma}{d\Omega}(\text{measured}) = \frac{d\sigma}{d\Omega}(\theta) + \frac{d\sigma}{d\Omega}(\pi - \theta) \quad \text{for } ^6\text{Li}(^6\text{Li}, ^6\text{Li}^*)^6\text{Li}^*$$

$$= \frac{d}{d\Omega}(\theta) \quad \text{for } ^6\text{Li}(^6\text{Li}, ^6\text{He})^6\text{Be}.$$

The derivation of the form factor for some of the exchange terms involves a 12-dimensional integral and to solve such an integral the interaction potential and wave functions are expanded in Gaussians and the integrals solved analytically. The expansion used for $V_{\text{eff}}$ is of the form

$$V_c(r_{ij}) = V_c \sum_n a_n e^{-b_n r_{ij}^2},$$

$$V_T(r_{ij}) = V_T \sum_m a_m (b_m r_{ij}^2) e^{-b_m r_{ij}^2}.$$

Since any reasonable functional form of the potentials can be expanded in terms of these Gaussians, we have chosen several for the central potential: the Yukawa potential with various depths and ranges,

$$V_c(r_{ij}) = v_c Y, \quad Y = e^{-br_{ij}}/_{br_{ij}},$$

or the long-range part of the Hamada-Johnston potential in the singlet-even and triplet-even states with a cutoff at $r_c = 1.05$ fm.[10] The fit of these potentials to a sum of four Gaussians is shown in Fig. 1. In the fit the strength, $S_c$, integrated out to 5 fm, is matched exactly:

$$S_c = \int_0^5 V_c(r) r^2 dr.$$

The shape of the short-range part of the potential has little effect on the form factor and does not need to be fitted well since the form factor is simply proportional to its strength, $S_c$. In contrast, the shape of the long-range part of the potential ($r \gtrsim 3$ or 4 fm) does affect the form factor. However, the long-range part contributes to the form factor more like $V_c(r)dr$ rather than $V_c(r)r^2dr$ and therefore contributes much less than the short-range part.

For the tensor interaction, the one-pion-exchange potential (OPEP) is used

$$V_T(r_{ij}) = v_T[1 + 3/br_{ij} + 3/(br_{ij})^2] Y,$$

with

$$b = 0.707 \text{ fm}^{-1},$$

$$v_T = 2.78 \text{ MeV}.$$

The value of $V_T$ is obtained from the pion-nuclear coupling constant of 0.08. The short-range part of the tensor potential contributes as $V_T(r)r^4$, and the strength function $S_T$ is defined

$$S_T = \int_0^4 V_T(r) r^4 dr,$$

where we have integrated out to 4 fm. $S_T$ is matched exactly in the fit to four Gaussians.

The radial wave functions are also expanded in terms of Gaussians. The form of the expansion for $(P^2)_{L=0}$ is

$$\mathfrak{A}(r_i, r_j) = N_i(\vec{r}_i \cdot \vec{r}_j) \sum_k a_k e^{-b_k r_i^2} \sum_l a_l e^{-b_l r_j^2},$$

where $N_i$ is a constant which properly normalizes the wave function. The wave function of a single $p$-shell nucleon bound to a $^5$Li or $^5$He core is calculated by assuming a Woods-Saxon shape for the single-particle potential. The depth of the well for the $^6$Li ground state is adjusted to give the

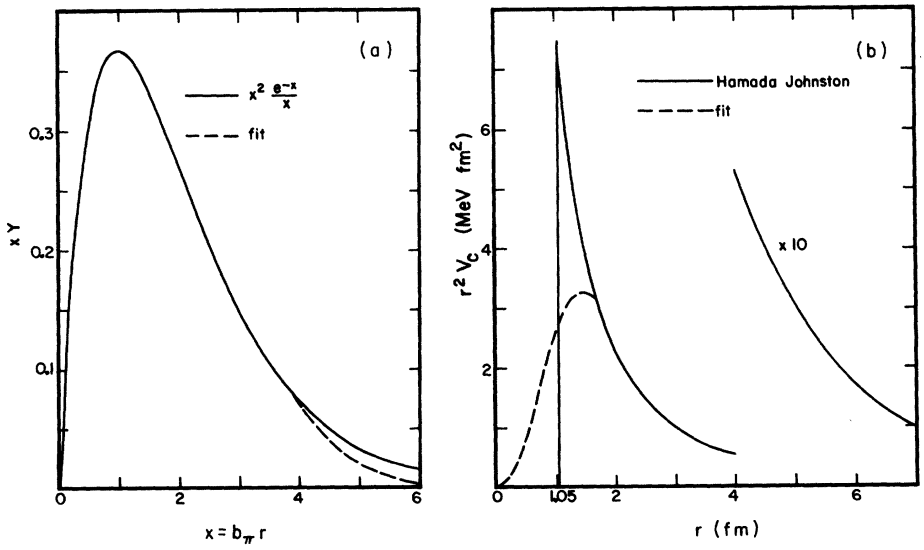


FIG. 1. (a) The Yukawa potential fitted with a sum of four Gaussians. The fit is nearly perfect for $x < 4$. (b) The Majorana potential obtained from the Hamada-Johnston potential, fitted to a sum of four Gaussians. The fit is nearly perfect for $2 \leq r \leq 7$ fm.

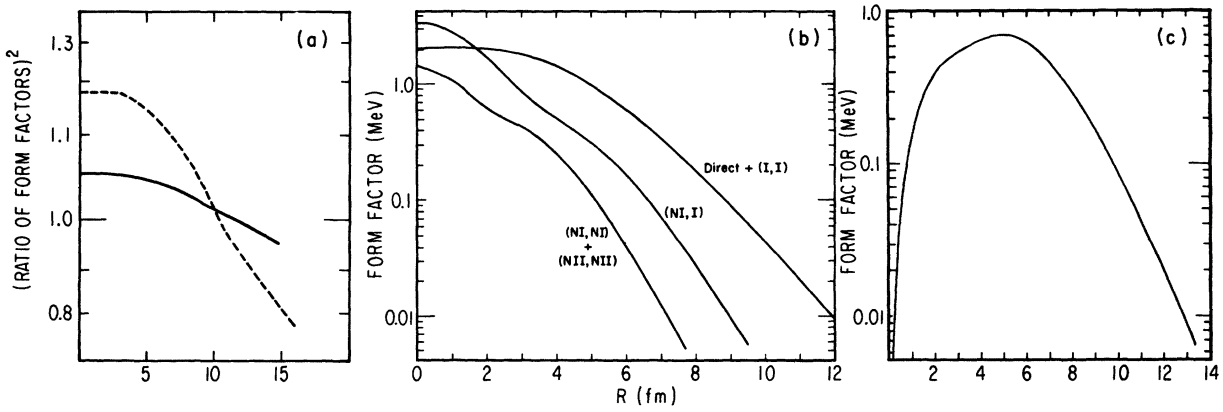


FIG. 2. (a) The ratio of the form factors squared. $^6$Li($^6$Li, $^6$Li*)$^6$Li*/$^6$Li($^6$Li, $^6$He)$^6$Be is plotted with $R$, the separation distance between the nuclei, using the wave functions described in the text (solid line), and using wave functions which have the experimental separation energies (dashed line). (b) The three componenets of the form factor for the central potential. Component 1 is the direct terms plus the terms involving the exchange of the two interacting nucleons (I, I). Component 2 is the terms involving the exchange of a noninteracting nucleon with an interacting nucleon (NI, I). Component 3 is the terms involving the exchange of both noninteracting nucleons (NI, NI) plus terms involving the complete exchange of the $p$-shell nucleons (NII, NII). The form factor is scaled by $(\frac{2}{3})^{1/2}$ to take care of the spin averaging and double counting. (c) The contribution to the tensor form factor using the OPEP form with total strength 3.7 MeV for the interaction. The form factor is scaled by $(\frac{10}{3})^{1/2}$ to take care of the spin averaging and double counting.

correct neutron separation energy. As an initial calculation it is reasonable to assume that the Coulomb interaction is the only difference between the three final states, and therefore the depth of the well is kept the same for all $p$-shell nucleons in the final nuclei. The depth is adjusted to give the correct neutron separation energy for $^6$He.

The Woods-Saxon solutions are fit to a series of three Gaussians. The fits are quite good,

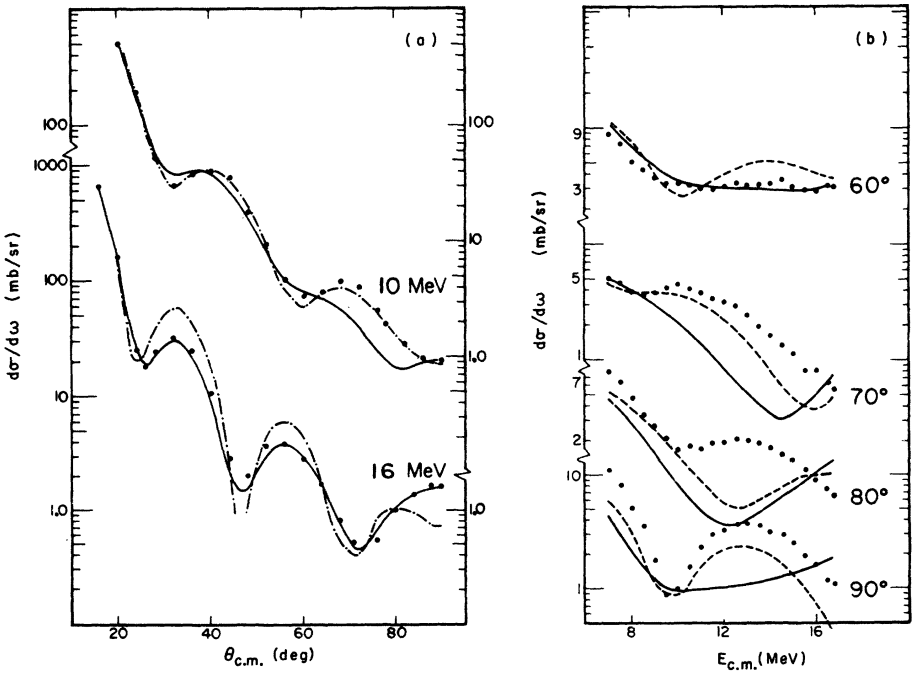


FIG. 3. The $^6$Li+$^6$Li elastic scattering data are fitted using optical potential 1.5 (solid line) and optical 1.6 (dashed line). The experimental excitation functions and 10-MeV angluar distribution are taken from Ref. 19. The 16-MeV data are taken from Ref. 17.

matching to within 1 or 2% out to distances of 11 to 14 fm. The accuracy of this Gaussian expansion is important because it means that the analytic solutions[7] to the form factors will be easily amenable to more accurate wave functions as they become available. The above calculation clearly underestimates the differences in the final-state nuclei. A major problem in obtaining a more accurate calculation is that the $^6$Be ground state is unstable to $\alpha$ plus two proton decay by 1.37 MeV whereas it is stable to single proton decay by 0.6 MeV. Some method needs to be found to treat a three-particle unbound system.

Using the wave functions and the Hamada-Johnston potential[10] the form factor is calculated and shown in Fig. 2. The figure conveys three messages. Figure 3(a) indicates that the ratio in the calculated form factors (solid line) for the $^6$Li-($^6$Li, $^6$Li*)$^6$Li* and the $^6$Li($^6$Li, $^6$He)$^6$Be reactions is near unity. However, if one allows the depth of the Woods-Saxon well to vary for the final nuclei to give the correct proton and/or neutron separation energies for all the nuclei, them a significantly larger deviation from unity is obtained (dashed line). This clearly indicates that differences in the form factors may be important and that more accurate calculations of differences between the wave functions is clearly needed. Figure 2(b) indicates that exchange terms involving noninteracting nucleons are clearly important and significantly alter the shape of the form factor. Figure 2(c) indicates that the radial dependence of the tensor form factor is very different from the shape of the central form factor. In studying Fig. 2 it is useful to know that the reaction is surfaced peaked, taking place primarily at a separation distance of about 5.6 fm. This is known from the Legendre polynomial expansion of the experimental data[11] and from the DWBA calculations shown later in this report.

## II. ELASTIC SCATTERING

Recently a fair amount of $^6$Li + $^6$Li elastic scattering eross-section measurements have been collected for bombarding energies $E_{\rm lab} \leq 32$ MeV, and analyzed using the optical model.[5, 12, 13] The analyses have given only fair agreement to the experimental data. The analyses of the elastic scattering data has been continued in this report and a total of 10 optical potentials have been obtained which are used in the DWBA.

The standard spin-independent optical potential used in the previous analyses and initially used in this analysis is of the form:

$$U(r) = -Vf(r) - iWg(r) + V_c(r),$$

where

$$f(r) = \{1 + \exp[(r - R_v)/a_v]\}^{-1}$$

and

$$g(r) = \{1 + \exp[(r - R_w)/a_w]\}^{-1}$$

for volume absorption. In one previous analysis[13] at energies $E_{\rm lab} < 20$ MeV a surface absorption was used but the fit using such a potential was unsatisfactory for the data at energies $E_{\rm lab} > 20$ MeV. The Coulomb potential is assumed to be due to a uniformly charged sphere of radius $R_c$. A standard optical-model code[14] has been altered to include Bose-Einstein statistics of the identical $^6$Li nuclei with spin 1.

Most of the earlier analyses have chosen $V$ and $W$ to be energy-independent. However, in this work a linear energy dependence has been allowed:

$$V \rightarrow V + V_E(E_{\rm c.m.} - 16.),$$

$$W \rightarrow W + W_E(E_{\rm c.m.} - 16.).$$

Combining the present results with previous work, Table II lists six optical potentials which give reasonable fits to the elastic scattering data at energies $15 \leq E_{\rm lab} \leq 36$ MeV. Figure 3 shows typical fits for two of the optical potentials.

To improve the optical-model description of the elastic scattering of two $^6$Li nuclei, a spin-orbit potential has been included in the scattering process. Such a potential couples the spin of each $^6$Li nucleus to the relative orbital angular momentum between the two nuclei. The strength of this potential is expected[15] to have an $A^{-1}$ dependence and is often neglected for nuclei heavier than a deuteron. The $A^{-1}$ dependence is expected from a microscopic description whereby each nucleon, in a nucleus with $A$ nucleons, has approximately $A^{-1}$ times the total angular momentum between the projectile and target. Using this $A^{-1}$ dependence, one would expect the strength

TABLE II. Optical-model parameters. Units are MeV, fm.

| Set | 1.1 [a] | 1.2 [b] | 1.3 | 1.4 | 1.5 | 1.6 |
|---|---|---|---|---|---|---|
| $R_V$ | 5.0 | 2.4 | 4.33 | 3.96 | 2.44 | 4.48 |
| $a_V$ | 0.460 | 1.15 | 0.524 | 0.520 | 0.835 | 0.613 |
| $R_W$ | 5.46 | 2.4 | 4.47 | 3.59 | 5.63 | 5.07 |
| $a_W$ | 0.728 | 1.15 | 0.673 | 0.935 | 0.701 | 0.591 |
| $V$ | 11.7 | 44.0 | 53.14 | 66.48 | 63.56 | 21.76 |
| $V_E$ | ... | −6.3 | +0.52 | +0.57 | +0.66 | −0.09 |
| $W$ | 6.9 | 28.0 | 12.51 | 15.17 | 5.08 | 8.71 |
| $W_E$ | ... | +1.13 | −0.25 | −0.48 | −0.40 | −0.29 |
| $R_c$ | 4.8 | 2.4 | 5.45 | 5.45 | 5.45 | 5.45 |

[a] Reference 12. [b] Reference 5.

of the spin-orbit potential to be comparable for $^6$Li and $^3$He since the spin-to-mass ratio is the same for these two nuclei. A recent study[16] of the $^3$He spin-orbital potential indicates that it is weak. However, analysis of the elastic scattering of $^4$He from $^6$Li, $^7$Li, and $^9$Be indicates that the inclusion of a moderately large target spin-orbit potential significantly improves the optical-model fits to the differential cross sections.[17] More work needs to be done to determine if the $A^{-1}$ rule is valid.

It is not the purpose of this work to learn anything about the strength of the $^6$Li spin-orbit potential. The inclusion of a spin-orbit potential will allow more freedom in choosing optical potentials to use in the DWBA calculations. It will be particularly interesting to see how the spin-orbit term affects the contribution of the tensor interaction to the inelastic cross sections. The tensor contribution comes from the $S=2$ channel which is most strongly affected by the spin-orbit potential.

In the $^6$Li + $^6$Li elastic scattering, the projectile spin-orbit and the target spin-orbit potentials are equal because of the identity of the two nuclei. Defining $\vec{I}$ as the projectile spin, $I'$ as the target spin, and $L$ as the relative angular momentum between the projectile and the target, the complete spin-orbit potential is:

$$V_{so} = v(r)\vec{L}\cdot\vec{I} + v'(r)\vec{L}\cdot\vec{I}',$$

$$v(r) = v'(r) = v_{so}(r),$$

$$V_{so} = v_{so}(r)\vec{L}\cdot\vec{S},$$

where $\vec{S}=\vec{I}+\vec{I}'$ is the channel spin. This potential commutes with $\vec{S}$, so that the eigenvalues of $S$ are good quantum numbers. Therefore it is convenient to describe the various spin states in terms of channel spin. The $^6$Li nucleus has spin 1 and $S=0, 1, 2$. The cross section amplitudes, $f_S(\theta)$, for the three channel spins, add incoherently

$$2\frac{d\sigma}{d\Omega} = \tfrac{1}{9}\,|f_{S=0}(\theta)+f_0(\pi-\theta)|^2 + \tfrac{3}{9}\,|f_1(\theta)-f_1(\pi-\theta)|^2 + \tfrac{5}{9}\,|f_2(\theta)+f_2(\pi-\theta)|^2.$$

The amplitudes are calculated using the same formulas as for a projectile with spin $S$ scattering off a spin-0 target. The radial form $v_{so}(r)$ of the optical potential has been chosen to be

$$v_{so}(r)\vec{L}\cdot\vec{S} = V_{so}\,\frac{2}{r}\,\frac{d}{dr}\,\{1+\exp[(r-R_s)/a_s]\}^{-1}\vec{L}\cdot\vec{S}.$$

Figure 4 and Table III show two fits to the data using the spin-orbit potential. The expected

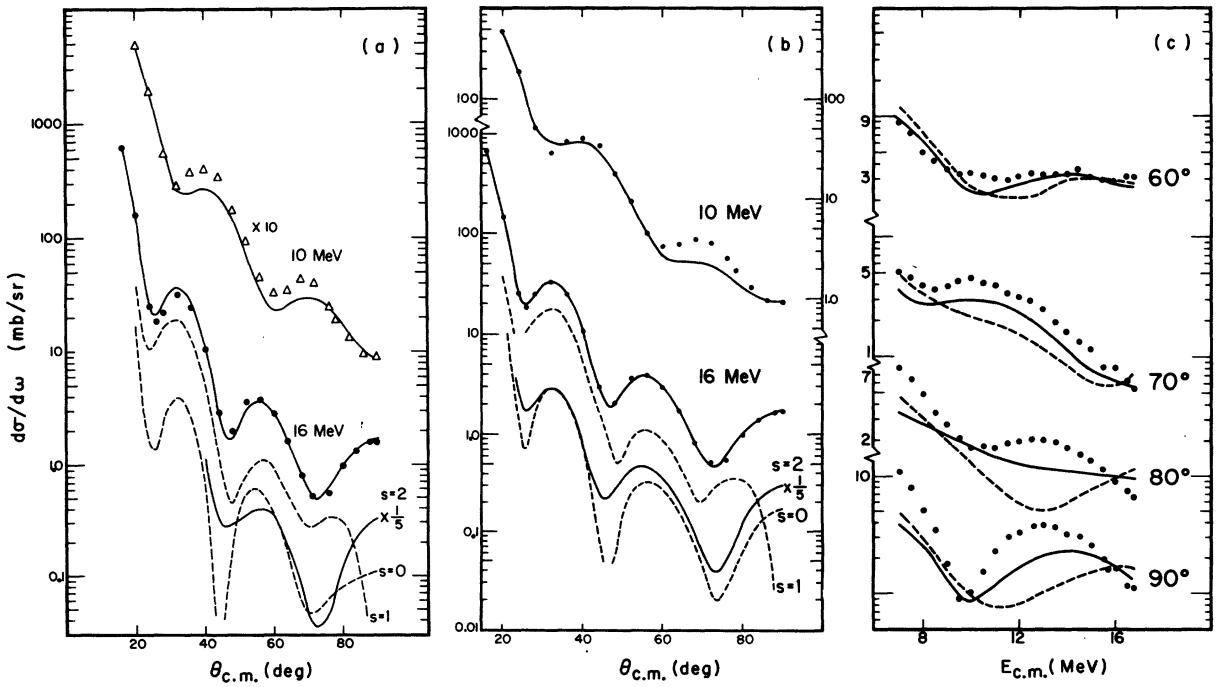


FIG. 4. The fits to the $^6$Li + $^6$Li elastic scattering data are shown for Set 2.1 [Fig. 4(a) and solid line in Fig. 4(c)] and Set 2.2 [Fig. 4(b) and dashed line in Fig. 4(c)]. The partial cross sections for channel spin $s=0, 1$ and 2 are shown for the $E_{c.m.}=16$ MeV fits.

strength of the spin-orbit potential according to the $A^{-1}$ rule is 1.5 to 2.0 MeV. The strength in these fits are 6.96 and 2.86 MeV, respectively. The diffuseness $a_s$ is smaller than is expected and there is more energy dependence, i.e., $V_E$ and $W_E$ are larger than they were in most of the previous fits.

The partial cross sections for the three channel-spin states $S=0, 1, 2$ are also shown in Fig. 5 for the fits at $E_{lab}=32$ MeV. Although both Sets 2.1 and 2.2 give nearly perfect fits to the 32-MeV data, the partial cross sections are significantly different. The importance of the spin-orbit potential is observed by comparing the $S=0$ partial cross section with $\frac{1}{5}$ of the $S=2$ partial cross section; the two should be equal if the spin-orbit potential is zero.

Both Sets 2.1 and 2.2 give better fits to the data than any of the previous six sets which indicates that the inclusion of the spin-orbit potential improves the fits. It is unclear whether the improvement is because the spin-orbit potential is important or whether it is simply a result of having more parameters to vary. Alternatively, there may be an $L$ dependence in the real potential which is partially simulated by the $L \cdot S$ potential.

An additional short-range repulsion was tried for the real part of the optical potential. Both the potentials calculated theoretically for heavy-ion scattering[18] and the analysis of the $\alpha$-$\alpha$ elastic scattering[19] data indicate a repulsive core is present. It was very easy to include such a term into the optical code and the DWBA code and this is primarily why it was tried. Unfortunately, a repulsive core would almost definitely be $L$-dependent but no allowance has been made for any $L$ dependence in the optical potential.

The repulsive soft core (s.c.) was taken to have a Woods-Saxon shape with a diffuseness of 0.1 fm

$$V_{sc}(r) = V_{sc}\{1+\exp[(r-R_{sc})/0.1]\}^{-1}.$$

Table IV gives two fits to the data. The inclusion of a repulsive core does not significantly improve the quality of the fits. Set 3.2 is interesting in that it is a "molecular"-type potential with a very shallow depth for the real part of the potential.

It appears that we are unable to satisfactorily describe the elastic scattering process. This will be the major weakness in our whole theoretical calculation. Fortunately we have 10 widely different sets of optical-model parameters which can be used in the DWBA calculations. It will probably be safe to assume that any results which are the same for all 10 sets are probably not seriously affected by errors in the optical potential. A possible way to improve the optical potential is to include $L$ dependence in the potential, but theoretical calculations are needed to predict what

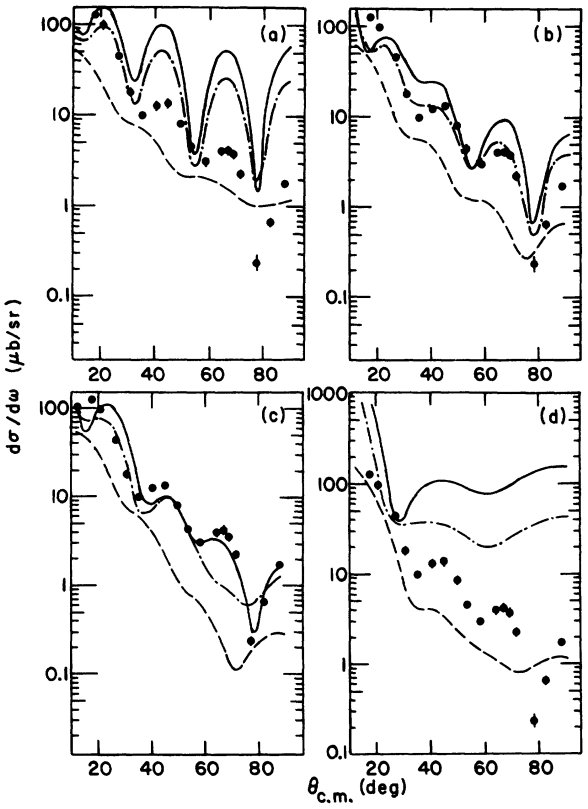


FIG. 5. The DWBA calculations of the $^6$Li($^6$Li, $^6$Li*)$^6$Li* reaction at $E_{lab}=32$ MeV are shown using four different optical potentials for the distorted waves: optical potentials 1.2 [Fig. 5(a)], 1.6 [Fig. 5(b)], 2.1 [Fig. 5(c)], and 3.2 [Fig. 5(d)]. The contribution of the tensor force (dashed line), and the incoherent sum of the tensor and central contributions with knock-on exchange (dashed-dotted line) and with additional full exchange for the central contribution (solid line) are shown. The experimental data with error bars shown are taken from Ref. 11.

TABLE III. Optical-model parameters. Units are MeV, fm.

| Set | $R_V$ | $a_V$ | $R_W$ | $a_W$ | $V$ | $V_E$ | $W$ | $W_E$ | Set | $R_{so}$ | $a_{so}$ | $V_{so}$ | $R_c$ |
|---|---|---|---|---|---|---|---|---|---|---|---|---|---|
| 2.1 | 3.78 | 0.579 | 3.63 | 0.870 | 112.0 | 2.20 | 18.84 | +0.42 | 2.1 | 4.56 | 0.277 | 6.96 | 5.45 |
| 2.2 | 3.07 | 0.827 | 4.94 | 0.771 | 50.6 | 3.56 | 8.01 | −0.40 | 2.2 | 4.54 | 0.253 | 2.86 | 5.45 |

TABLE IV. Optical-model parameters. Units are MeV, fm.

| Set | $R_V$ | $a_V$ | $R_W$ | $a_W$ | $V$ | $V_E$ | $W$ | $W_E$ | Set | $R_{sc}$ | $V_{sc}$ | $R_{sc}$ |
|---|---|---|---|---|---|---|---|---|---|---|---|---|
| 3.1 | 3.22 | 0.700 | 4.71 | 0.957 | 54.1 | +0.87 | 6.96 | +0.10 | 3.1 | 2.00 | 50.0 | 5.45 |
| 3.2 | 5.83 | 0.862 | 6.42 | 0.448 | 4.16 | +0.01 | 2.30 | +0.14 | 3.2 | 1.93 | 30.5 | 5.45 |

form the $L$ dependence should take. One possibility is to allow a different imaginary potential for the even and odd partial waves to simulate the different reaction channels which are available to the even and odd momentum states. This has been shown to be important in some elastic scattering reactions, such as $^3$He-$^3$He elastic scattering.[20]

## III. DWBA CALCULATIONS

The DWBA calculations were performed using the program DWUCK[21] which was altered slightly to treat the identical $^6$Li nuclei correctly. Using the form factors calculated with the Hamada-Johnston potential for the central interaction and the OPEP form for the tensor interaction, the $^6$Li($^6$Li, $^6$Li*)$^6$Li* and $^6$Li($^6$Li, $^6$He)$^6$Be cross sections are calculated with each of the 10 sets of optical potentials given in the previous section. It should be emphasized that there are no free parameters and even the magnitude of the cross section is determined. Figure 5 shows the calculations which give the best and the worst agreement with the data.[10] The calculations including all exchange terms, and the calculations including only the exchange terms involving the interacting nucleons (knock-on exchange) are shown. The knock-on exchange terms increase the cross section by a factor of 4, but do not change the shape of the angular distributions, because the form factors for the direct and knock-on exchange terms are assumed to be identical. The inclusion of all exchange terms increase the cross section by nearly an order of magnitude over the direct without-exchange cross section. The contribution of the tensor interaction with knock-on exchange is also shown.

All of the calculations, except those with optical-potential Sets 3.1 and 3.2 which have repulsive cores, agree remarkably well with the data at angles backward of 35° c.m. In particular, the locations of the maxima and minima agree to within a few degrees. In contrast, none of the calculations describe the data forward of 35° c.m. In fact, every calculation except Set 3.2 gives a maximum between 20 and 26° c.m. and a minimum near 15° c.m., which is in poor agreement with the data which is still rising at 17.5° c.m. Set 3.2, which is unique in that it has a very shallow "molecular"-type potential, does not have a minimum at 15° but does poorly at the backward angles.

A comparison of the magnitude of the cross sections of each calculation with the data indicates that except for Sets 1.2 and 3.2, part or all of the strength from the exchange terms must be included to give the right magnitude. Sets 1.2 and 3.2 have approximately the correct magnitude using only the direct contribution. The tensor contribution is less than 30% of the total cross section in all cases. The inclusion of a spin-orbit potential in Set 2.1 does not affect the tensor contribution much, except to make if more forward peaked.

Calculations have also been performed using a Yukawa $N$-$N$ interaction of range 1 fm, 1.1 fm, and 1.41 fm. These calculations also show a

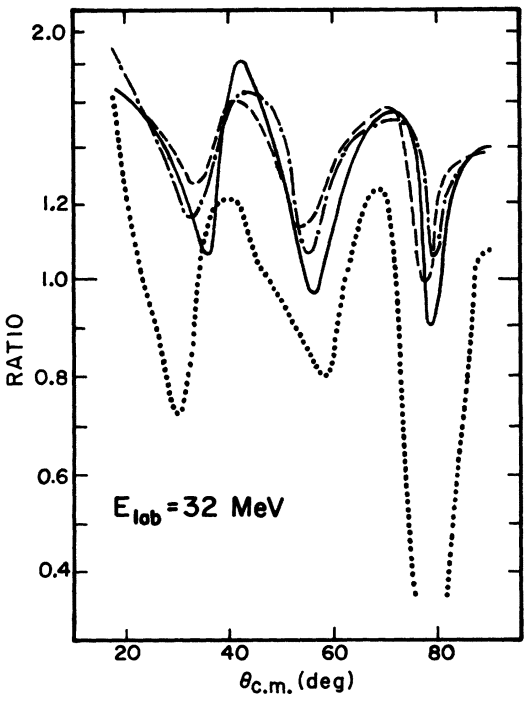


FIG. 6. The ratio of the $^6$Li($^6$Li, $^6$Li, *)$^6$Li*/$^6$Li($^6$Li, $^6$He)-$^6$Be differential cross sections at $E_{lab}$=32 MeV is obtained from Ref. 17 by fitting the experimental angular distributions with even Legendre polynomials (dotted line). This is compared with the DWBA calculations using optical potentials 1.3 (dashed line) and 1.6 (dashed-dotted line) both with knock-on exchange in the form factor and using potential 2.1 and full exchange in the form factor (solid line).

minimum near 15° c.m. with a maximum between 20 and 26° c.m. for all optical-model sets except Set 3.2. Most of the fits using a Yukawa interaction do slightly worse at backward angles.

In Fig. 6, the experimental ratio of the $^6$Li-($^6$Li, $^6$Li*)$^6$Li* to the $^6$Li($^6$Li, $^6$He)$^6$Be differential cross section obtained from a Legendre polynomial expansion[11] of the data is compared to the theoretical calculations using the three sets of optical-model parameters which give the best agreement with the experimental angular distributions. The experimental ratio fluctuates with angle, having several maxima and minima and varying from 1.63 at 17.4° to 0.17 at 78.8°. The calculated ratios also vary with angle and the agreement with the experimental fluctuation in the ratio is directly correlated to how well the calculation reproduces the $^6$Li($^6$Li, $^6$Li*)$^6$Li* cross section. This correlation is not surprising when one realizes that the fluctuation in the ratio is a result of the $^6$Li-($^6$Li, $^6$Li*)$^6$Li* diffraction pattern being shifted with respect to the $^6$Li($^6$Li, $^6$He)$^6$Be diffraction pattern.

The calculated ratio is consistently much larger than the experimental ratio at all angles. There are three differences in the calculation of the cross sections for the two reactions which cause their calculated ratio to differ from unity:

(i) Differences in the Coulomb interaction in the outgoing channel

$ZZ' = 9$ for $^6$Li* + $^6$Li*

$= 8$ for $^6$He + $^6$Be;

(ii) differences in the kinetic energy in the outgoing channel, resulting from the $Q$-value difference

$Q = -7.12$ MeV for $^6$Li($^6$Li, $^6$Li*)$^6$Li*

$= -7.8$ MeV for $^6$Li($^6$Li, $^6$He)$^6$Be;

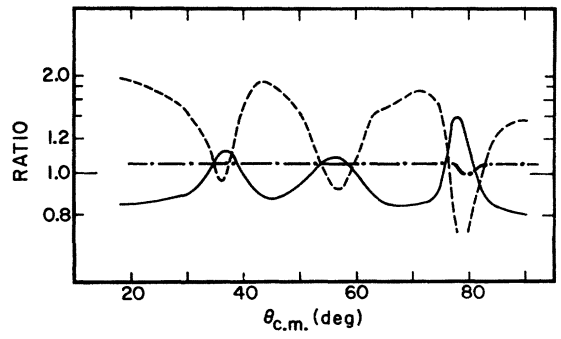


FIG. 7. The ratio of the $^6$Li($^6$Li, $^6$Li*)$^6$Li* cross section to the $^6$Li($^6$Li, $^6$Li*)$^6$Li* altered cross section at $E_{lab} = 32$ MeV where the latter is altered separately by using the $^6$He + $^6$Be Coulomb interactions (solid line), the $^6$Li($^6$Li, $^6$He)$^6$Be $Q$ value (dashed line), and the $^6$Li($^6$Li, $^6$He)-$^6$Be form factor (dashed-dotted line).

(iii) differences in the form factors because of the different wave functions for $^6$Li*, $^6$He, and $^6$Be.

The importance of these three differences can be studied separately by recording the ratio of the $^6$Li($^6$Li, $^6$Li*)$^6$Li* total cross section to the $^6$Li($^6$Li, $^6$Li*)$^6$Li* altered cross section where the latter is altered separately by using the $^6$He + $^6$Be Coulomb interaction, the $^6$Li($^6$Li, $^6$He)$^6$Be $Q$ value, and its form factor. At $E_{lab} = 32$ MeV these ratios are

$$\frac{\sigma(^6\text{Li}^*)}{\sigma(^6\text{Li}^*)_{\text{altered}}} = \begin{cases} 0.88 \pm 0.01 \text{ Coulomb} \\ 1.60 \pm 0.05 \ Q \text{ value} \\ 1.026 \pm 0.002 \text{ form factor}. \end{cases}$$

The errors in these numbers give the variation of these ratios with different optical potentials. As is seen, all differences are only weakly dependent upon the optical potential.

In Fig. 7 we plot how these three differences affect the angular dependence of the ratio using optical potential Set 2.1. As expected, the Coulomb and the $Q$-value differences partially cancel (the smaller Coulomb barrier for the $^6$He + $^6$Be channel partially compensates for the larger negative $Q$ value) but the $Q$-value difference dominates giving a ratio much larger than unity.

In Fig. 8 the $^6$Li($^6$Li, $^6$Li*)$^6$Li* data at $E_{lab} = 36$ MeV is plotted along with three calculations using optical potential Sets 1.3, 1.6, and 2.1. These three sets were chosen because they gave the best agreement with the 32-MeV data. In looking

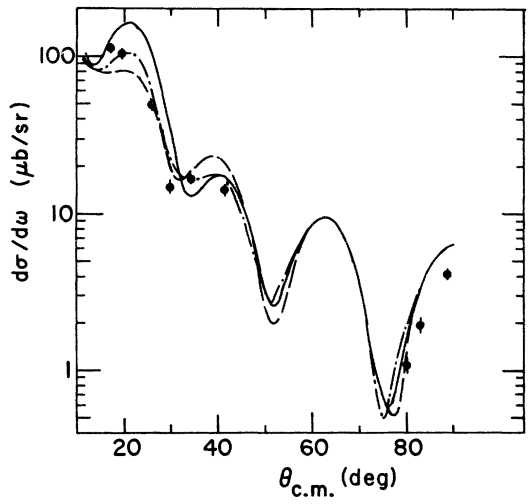


FIG. 8. The DWBA calculation of the $^6$Li($^6$Li, $^6$Li*)$^6$Li* angular distribution at $E_{lab} = 36$ MeV using optical potentials 1.3 (dashed line) and 1.6 (dashed-dotted line) both with knock-on exchange and Set 2.1 with full exchange (solid line). The data with error bars are taken from Ref. 17.

at the 36-MeV data, our main concern is the way the cross section changes with energy. All three calculations predict approximately a 50% rise in the differential cross section at forward angles as the bombarding energy increases from 32 to 36 MeV. In contrast the data indicate the cross section is not rising significantly. All three calculations show that the minimum near 35° shifts forward 3 or 4° as the energy increases from 32 to 36 MeV. This is in agreement with the data which shows a minimum at 35° at $E_{lab} = 32$ MeV and a minimum at 31 or 32° at $E_{lab} = 36$ MeV. The calculations are in closer agreement with the forward angular distribution at 36 MeV than they are at 32 MeV. Also the three calculations show a deep minimum near 78°. in apparent agreement with the incomplete data.

In Fig. 9 the ratios of the $^6$Li($^6$Li, $^6$Li*)$^6$Li*/ $^6$Li($^6$Li, $^6$He)$^6$Be cross sections at $E_{lab} = 36$ MeV are plotted along with the calculations using optical-model Sets 1.3, 1.6, and 2.1. Similar to the ratios at $E_{lab} = 32$ MeV, the calculated ratios are 15 to 20% higher than the experimental ratio. The oscillatory structure in the calculated ratio at forward angles agrees fairly well with the data. This is not surprising because the calculations are in fair agreement with the forward angle angular distributions. The ratio at 80° c.m. is particularly interesting because at $E_{lab} = 32$ MeV the experimental ratio is 0.2 at 80° and at $E_{lab} = 36$ MeV the ratio is 3.2 at 80°. This is a factor of 16 change as the center-of-mass energy changes by only 2 MeV. The calculations shown here do not reproduce this strong energy dependence. However, it was found that slight differences between optical potentials in the $^6$Li*-$^6$Li* and $^6$He-$^6$Be outgoing channels significantly affect the ratio and cross sections at backward angles. A 1% change in the depth of the real and imaginary Woods-Saxon well can lead to much improved agreement between theory and the data for the angular and energy dependence of the ratio at backward angles without affecting the calculated ratio at forward angles.

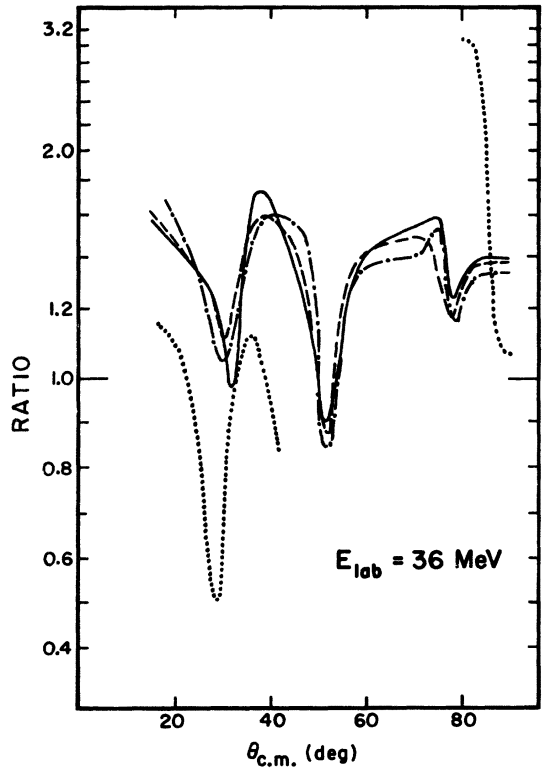


FIG. 9. The ratio of the $^6$Li($^6$Li,$^6$Li*)$^6$Li*/$^6$Li($^6$Li,$^6$He)-$^6$Be experimental angular distributions at $E_{lab} = 36$ MeV taken from Ref. 17 is compared to DWBA calculations using optical potentials 1.3 (dashed line) and 1.6 (dashed-dotted line) both with knock-on exchange and potential 2.1 with full exchange (solid line).

In Fig. 10(a) the excitation function of the $^6$Li-($^6$Li, $^6$Li*)$^6$Li* cross section near 90° is plotted along with the calculations using optical-model Sets 1.3, 1.6, and 2.1. All three calculations reproduce the trend of the data reasonably well. In Fig. 10(b) the excitation function of the ratio of the two cross sections near 90° c.m. is plotted along with the calculations using optical-model Sets 1.3, 1.6, and 2.1. As in previous instances the calculated ratio is considerably larger than the experimental ratio.

## IV. DISCUSSION

### A. Agreement between the theory and the data

The agreement between the calculations and the data at backward angles, $\theta_{c.m.} > 35°$, is remarkably good. Most calculations agree well with the magnitude and the angular and energy dependence of the backward-angle cross sections, and do an excellent job of reproducing the oscillatory structure in the ratio of the $^6$Li($^6$Li, $^6$Li*)$^6$Li*/ $^6$Li($^6$Li, $^6$He, )$^6$Be cross sections. Even if most of the optical sets give a poor description of the true optical potential, a point has been proven. Much of the data is capable of being described within the direct-reaction DWBA theory, and this is evidence that these reactions are proceeding nearly entirely by a direct mechanism at backward angles. It is unlikely that the DWBA without any free parameters could describe the data so well, if this were not the case.

It is of significance that many of the calculations predict the deep minimum in the $^6$Li-($^6$Li, $^6$Li*)$^6$Li* cross section near 80° at $E_{lab} = 32$ and 36 MeV. It is at this deep minimum that compound-nuclear processes or possibly multistep

processes would become important if they are present. In fact it was originally our impression that multistep processes are important at this minimum and that an accidental cancellation of two amplitudes from two different processes were occurring for the $^6$Li($^6$Li, $^6$Li*)$^6$Li* reaction causing it to have a much smaller cross section at this minimum. This original impression now appears to be incorrect because the DWBA calculations generally predict a deep minimum at 80° and $E_{lab} = 32$ and 36 MeV for the $^6$Li($^6$Li, $^6$Li*)-$^6$Li* reaction. All calculations also predict qualitatively that the minimum in the $^6$Li($^6$Li, $^6$He)$^6$Be cross section is shallower than the minimum in the $^6$Li($^6$Li, $^6$Li*)$^6$Li* cross section at 32 MeV, but quantitatively the $^6$Li($^6$Li, $^6$He)$^6$Be minimum is not shallow enough.

The calculations also predict the approximate magnitude of the cross sections. Unfortunately it is difficult to reach any definite conclusions from this because the magnitudes of the cross sections vary considerably with the optical potential, and there is also an uncertainty as to the importance of the exchange terms which change the calculated magnitude by nearly an order of magnitude.

It has been suggested[22] that the excellent agreement between theory and experiment is simply an indication that the DWBA calculations have correctly predicted the few angluar momenta which enter into the scattering process. These angular momenta, $L = 6$ or 8 (odd $L$ are forbidden) corresponds to the angular momenta of a grazing collision and may be characteristic of several kinds of reaction processes. It is unlikely that simply choosing the correct momenta will account for all the agreement between theory and experiment, and in particular the main argument against this suggestion is the fine agreement between theory and experiment for the magnitude of the cross sections.

### B. Disagreement between the calculations and the data

There is poor agreement between the calculations and the data at forward angles $\theta_{c.m.} \leq 35°$, with the calculation failing to predict the energy dependence of the cross section or the location of the maxima and minima in the angular distributions. This disagreement at forward angles is similar to the anomaly found in the angular dis-

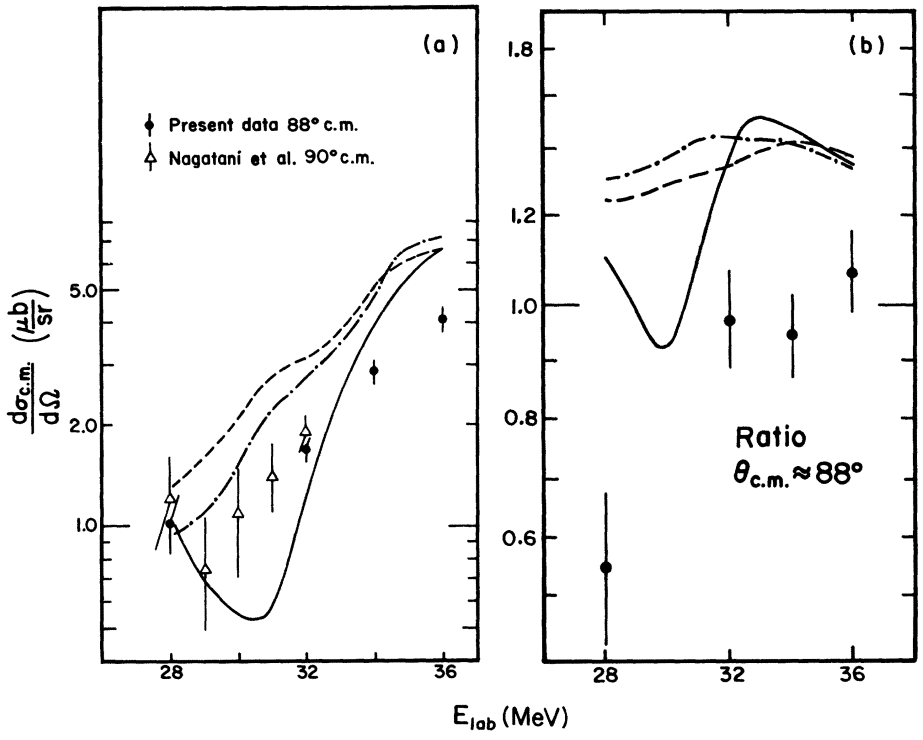


FIG. 10. The experimental excitation function of the $^6$Li($^6$Li, $^6$Li*)$^6$Li* reaction [Fig. 10(a)] and to the ratio of the differential cross sections $^6$Li($^6$Li, $^6$Li*)$^6$Li*/$^6$Li($^6$Li, $^6$He)$^6$Be [Fig. 10(b)] at about 90° in the center of mass are compared to the DWBA calculations using optical potential 1.3 (dashed-dotted line) and 1.6 (dashed line) both with knock-on exchange and potential 2.1 and full exchange (solid line). The data represented by triangles is taken from Ref. 4 and the data represented by solid circles is taken from Ref. 17.

tributions of the ($^3$He, $t$) reactions,[23] and may result from the presence of two-step processes such as a stripping reaction followed by a pickup reaction.

The second major disagreement is the large discrepancy between the experimental and calculated ratios for the $^6$Li($^6$Li, $^6$Li*)$^6$Li*/ $^6$Li($^6$Li, $^6$He)$^6$Be cross sections. The calculated ratio is 15–20% larger than the experimental ratio at nearly all angles and energies. Furthermore this disagreement persists no matter which optical potential is used. The major problem with calculating the ratio of the two cross sections is determining differences in the nucleon wave functions of the three final-state nuclei, $^6$He, $^6$Li*(3.56), and $^6$Be. In the calculation of the form factor used here, only first-order differences due to the Coulomb interaction have been considered. This calculation clearly has underestimated the differences in the wave functions and has made the $^6$Be particle stable where in reality it is unstable to $\alpha + 2p$ decay by 1.37 MeV. The experimental ratio of the cross sections may be a very powerful tool for probing differences in the $^6$He, $^6$Be, and $^6$Li* wave functions.

Another possible solution to the disagreement between the theoretical and experimental ratio of the cross sections is that the optical potential in the outgoing $^6$Li* + $^6$Li* and $^6$He + $^6$Be channels is different. In particular $^6$Be, being unbound, has a long tail which could alter the optical potential. Also it has been observed[7] that differences in the real and imaginary well depths of the optical potential in the two outgoing channels can lead to improved agreement between theory and the data for the angular and energy dependence of the ratio at backward angles.

### C. Exchange terms

Because of the uncertainty in the optical potential and the large fluctuation in the magnitudes of the calculated cross sections using various optical-potential sets, it is difficult to say anything concrete about the importance of exchange terms. The calculations which give the best agreement to the data have part or all of the exchange terms included. This is the only experimental indication that exchange terms are important.

We know from ($p, p'$) microscopic analyses[24] that exchange terms are sometimes important. For example the microscopic analysis[25] of the $^{40}$Ca($p, p'$) indicates that the inclusion of knock-on exchange increases the cross sections by factors of 2 to 7 and their inclusion correctly predicts the magnitude of the experimental cross sections. This work was particularly significant because the wave functions used in the calculation are well known and agree well with the form factors obtained from electron scattering. Although the DWBA does not treat exchange terms correctly, the success of the microscopic ($p, p'$) calculations indicates that this may not be a serious problem.

Our study finds that the exchange terms involving noninteracting nucleons also have a significant effect on the cross sections. Although they are not as important as the knock-on exchange terms, they change the $^6$Li($^6$Li, $^6$Li*)$^6$Li* and the $^6$Li($^6$Li, $^6$He)$^6$Be cross sections by factors of almost 2. We have included only exchange between the $p$-shell nucleons and have not looked at exchange with the 1$S$ nucleons. The exchange with the 1$S$ nucleons may also be important because of their large number. However, because the 1$S$ nucleon wave functions are of much shorter range than the $p$-shell nucleon wave functions these exchange terms are probably less important than the ones that have been considered.

This study has treated exchange terms nearly exactly within the DWBA framework except for recoil effects which have been neglected. The importance of recoil effects in these reactions must be investigated further.

### D. Tensor interaction

The contribution of the tensor force to the $^6$Li($^6$Li, $^6$Li*) $^6$Li and the $^6$Li($^6$Li, $^6$He)$^6$Be reactions is calculated to be less than 30% of the total cross section using the strength obtained from the pion-nucleon coupling constant. Experimentally the tensor contribution is expected to be small because of the deep minimum near 78°. If the contribution of the tensor force is sizable, the deep minimum at 78° would likely not occur. The tensor force's contribution is almost certainly smoothly varying with angle because of the coherent contribution of five-spin states and its incoherence with the contribution of the central force. These results are taken as evidence against a strong tensor interaction, such as that used to analyze the $^{54}$Fe($^3$He, $t$)$^{54}$Co reaction.[26] Although the tensor contribution is small, it is more forward peaked than the contribution of the central forces, and its inclusion in the DWBA calculation significantly improves the agreement with the data at forward angles. The data at forward angles and the data at the minimum near 78° collectively suggest that the strength of the tensor force used in these calculations is approximately correct. It therefore is reasonable to conclude that the "effective" tensor interaction between nucleons in nuclear matter is not much

different than the tensor interaction between free nucleons.

### E. Other microscopic calculations

If the concept of an effective $N$-$N$ interaction is to have any real meaning, it must be the same for all types of reactions. The microscopic analysis of some reactions, such as ($^3$He, $t$), have run into serious problems and the study of the $^6$Li-($^6$Li, $^6$Li*)$^6$Li* and the $^6$Li($^6$Li, $^6$He)$^6$Be reaction can be a useful way to amplify and expand on these problems. For example, the poor agreement between theory and experiment at forward angles for some ($^3$He, $t$) reactions[22] has also appeared in the present analysis of the $^6$Li($^6$Li, $^6$Li*)$^6$Li* and $^6$Li($^6$Li, $^6$He)$^6$Be reactions.

Many of the inelastic proton reactions have been analyzed microscopically using a Yukawa interaction. In particular Austin[1] has analyzed ($p, p'$) experiments in the 10–55 MeV energy range, and using a Yukawa interaction of range 1 fm, he obtained a strength of $12 \pm 2.5$ MeV for $V_{11}$ which was nearly independent over the energy range 10–52 MeV. He included knock-on exchange in his calculations. Bray *et al.*,[27] who have made a similar analysis of the $^6$Li($p, p'$)$^6$Li*(3.56) reaction, obtained a value of $V_{11} = 8.76$ MeV at $E_p = 25.9$ MeV and $V_{11} = 10.6$ MeV at $E_p = 45.4$ MeV. These fluctuations in the extracted values of $V_{11}$ and its energy dependence result primarily from variations in the optical potentials used in the DWBA calculations. The optical potential is much less accurately known for the $^6$Li($^6$Li, $^6$Li*)$^6$Li* reaction and the large variation in our extracted values of $V_{11}$ indicate this. Our results using a 1 fm range Yukawa with no exchange, knock-on exchange, and full exchange are shown in Table V. The results of Clement and Perez,[5] who used optical Set 1.2, agree with our results using the same optical set if the data they used are normalized to ours.

TABLE V. Values of $V_{11}$ (MeV) using a 1.0-fm-range Yukawa.

| Optical set | With full exchange | With knock-on exchange | With no exchange |
|---|---|---|---|
| 1.1 | 6.2 | 9.4 | 18.8 |
| 1.2 | 2.9 | 4.5 | 9.0 |
| 1.3 | 6.5 | 9.6 | 19.2 |
| 1.4 | 6.1 | 9.1 | 18.2 |
| 1.5 | 6.5 | 9.3 | 18.6 |
| 1.6 | 6.5 | 9.5 | 19.0 |
| 2.1 | 8.3 | 11.5 | 23.0 |
| 2.2 | 6.8 | 10.0 | 20.0 |
| 3.1 | 5.2 | 7.6 | 15.2 |
| 3.2 | 2.2 | 3.7 | 7.4 |

The fluctuation of $V_{11}$ for various optical-model sets makes a meaningful comparison with the ($p, p'$) studies difficult. Much more needs to be learned about the elastic wave functions (or the optical potential) before accurate information concerning the strengths of the $N$-$N$ interaction can be obtained. However the situation is not as bad as it may seem because it is reasonable to reject three of the potentials. Potential Sets 3.1 and 3.2, which have a repulsive core, do very poorly describing the inelastic cross sections. The Clement and Perez optical Set 1.2 is very energy dependent and does a poorer job of fitting the elastic cross sections than do the others. With these three potentials eliminated the strength of $V_{11}$ using knock-on exchange is:

$$V_{11} = 10.3 \pm 1.2 .$$

*Work supported in part by the U. S. Atomic Energy Commission.

[1] *The Two-Body Force in Nuclei*, edited by S. M. Austin and G. M. Crawley (Plenum, New York, 1972).

[2] P. G. Roos, in *The Two-Body Force in Nuclei*, (see Ref. 1), p. 333.

[3] V. I. Chuev, V. V. Davydov, V. I. Manko, B. G. Novatsky, S. B. Sakuta, and D. N. Stepanov, Phys. Lett. 31B, 624 (1970).

[4] K. Nagatani, D. P. Boyd, P. F. Donovan, E. Beardsworthy, and P. A. Assimakopoulos, Phys. Rev. Lett. 24, 675 (1970).

[5] C. F. Clement and S. M. Perez, Nucl. Phys. A196, 561 (1972).

[6] A. N. Boyarkina, Izv. Akad. Nauk SSSR Ser. Fiz. 28, 337 (1964) [transl.: Bull. Acad. Sci. USSR Phys. Ser. 28, 255 (1964)].

[7] W. R. Wharton, Ph.D. thesis, University of Washington, Seattle, 1972 (unpublished).

[8] H. A. Bethe, in *The Two-Body Force in Nuclei*, (see Ref. 1), p. 138.

[9] R. C. Johnson, in *Polarization Phenomena in Nuclear Reactions*, edited by H. H. Barschall and W. Haeberli (University of Wisconsin, Madison, 1970), p. 143; P. Schwandt and H. Haeberli, Nucl. Phys. A123, 401 (1969); H. Cords, G. U. Din, M. Ivanovich, and B. A. Robson, Nucl. Phys. A113, 608 (1968).

[10] T. Hamada and I. D. Johnston, Nucl. Phys. 34, 382 (1962); S. A. Moskowski and B. L. Scott, Ann. Phys. (N.Y.) 11, 65 (1960).

[11] W. R. Wharton, J. G. Cramer, D. H. Wilkinson, J. R. Calarco, and K. G. Nair, preceding paper, Phys. Rev.

C 9, 156 (1974).
[12]H. T. Fortune, G. C. Morrison, and R. H. Siemssen, Phys. Rev. C 3, 2116 (1971).
[13]Gernot Gruber, M. S. thesis, University of Heidelberg, 1971 (unpublished).
[14]W. R. Smith, *Elastic Scattering Search Program*, University of Southern California, Nuclear Physics Laboratory (unpublished) [AEC Contract A. T. (04-3)-136 Feb. 1967].
[15]H. Feshbach, Ann. Rev. Nucl. Sci. 8, 49 (1958).
[16]D. M. Patterson, Ph.D. thesis, University of Washington, 1971 (unpublished).
[17]H. G. Bingham, K. W. Kemper, and N. R. Fletcher, Nucl. Phys. A175, 374 (1971).
[18]R. H. Siemssen, in Nuclear Spectroscopy II, edited by J. Cerny (Academic, New York, to be published), Chap. IV.
[19]S. A. Ofzal, A. A. Z. Ahmed, and S. Ali, Rev. Mod. Phys. 41, 247 (1969).
[20]D. R. Thompson, Y. C. Yang, J. A. Koepka, and R. E. Brown, Nucl. Phys. A201, 301 (1973).
[21]DWUCK version—8 August 1969, by P. D. Kunz, Department of Physics, University of Colorado, Boulder, Colorado 80302.
[22]J. S. Blair, private communication.
[23]J. R. Comfort, J. P. Schiffer, A. Richter, and M. M. Stautberg, Phys. Rev. Lett. 26, 1338 (1971).
[24]J. D. Perez, Nucl. Phys. A191, 19 (1972).
[25]R. Schaffer, Nucl. Phys. A132, 186 (1969).
[26]E. Rost and P. D. Kunz, Phys. Lett. 30B, 231 (1969).
[27]K. H. Bray, M. Jain, K. S. Jayaraman, G. Lobianco, G. A. Moss, W. T. H. Van Oers, D. O. Wells, and F. Petrovich, Nucl. Phys. A189, 35 (1972).